

Caspase-9 regulates apoptosis/proliferation balance during metamorphic brain remodeling in *Xenopus*

Laurent Coen, Karine Le Blay, Isaline Rowe, and Barbara A. Demeneix*

Evolution des Régulations Endocriniennes, Muséum National d'Histoire Naturelle, Unité Mixte de Recherche–Centre National de la Recherche Scientifique 5166, Unité Scientifique du Muséum 501, Paris, France

Edited by Donald D. Brown, Carnegie Institution of Washington, Baltimore, MD, and approved March 23, 2007 (received for review October 6, 2006)

During anuran metamorphosis, the tadpole brain is transformed producing the sensorial and motor systems required for the frog's predatory lifestyle. Nervous system remodeling simultaneously implicates apoptosis, cell division, and differentiation. The molecular mechanisms underlying this remodeling have yet to be characterized. Starting from the observation that active caspase-9 and the Bcl-X_L homologue, XR11 are highly expressed in tadpole brain during metamorphosis, we determined their implication in regulating the balance of apoptosis and proliferation in the developing tadpole brain. *In situ* hybridization showed caspase-9 mRNA to be expressed mainly in the ventricular area, a site of neuroblast proliferation. To test the functional role of caspase-9 in equilibrating neuroblast production and elimination, we overexpressed a dominant-negative caspase-9 protein, DN9, in the tadpole brain using somatic gene transfer and germinal transgenesis. In both cases, abrogating caspase-9 activity significantly decreased brain apoptosis and increased numbers of actively proliferating cells in the ventricular zone. Moreover, overexpression of XR11 with or without DN9 was also effective in decreasing apoptosis and increasing cell division in the tadpole brain. We conclude that XR11 and caspase-9, two key members of the mitochondrial death pathway, are implicated in controlling the proliferative status of neuroblasts in the metamorphosing *Xenopus* brain. Modification of their expression during the critical period of metamorphosis alters the outcome of metamorphic neurogenesis, resulting in a modified brain phenotype in juvenile *Xenopus*.

cell proliferation | mitochondrial apoptotic pathway | *Xenopus* metamorphosis | XR11/Bcl-XL | germinal transgenesis

Thyroid hormone-induced anuran metamorphosis is marked by dramatic morphological remodeling and physiological changes in most of the tadpole tissues. Brain morphology alters radically as the tadpole changes from an herbivorous, swimming organism to a predatory frog (1). However, beyond the basic fact that remodeling of the CNS during metamorphosis involves cell-specific decisions inducing apoptosis, cell division, and differentiation, little data exist on where and how these processes are regulated. This is particularly true for neuronal apoptosis and the mechanisms regulating proliferation/apoptotic balance in the metamorphosing CNS.

Apoptosis is an evolutionary well conserved mechanism, essential for maintenance of tissue homeostasis and correct development of all multicellular organisms (for review see ref. 2). Two major apoptotic death pathways have been characterized, the extrinsic pathway triggered by membrane death receptors and the intrinsic pathway initiated in mitochondria (2). Apoptosis initiated by the mitochondrial pathway predominates in the developing brain (3, 4), and cell death in neurodegenerative disorders is directly or indirectly regulated by this pathway (5, 6). Further, phenotypes produced by inactivation of key apoptotic genes in mice, show an overriding role of the mitochondrial death route in neural development (7, 8).

The intrinsic mitochondrial pathway implicates conserved mechanisms involving proteases, called caspases (9, 10), and regulatory pro- and antiapoptotic mitochondrial factors (11, 12). These factors

include the Bcl-2 family that are either proapoptotic (such as Bax) or antiapoptotic (such as Bcl-2), with the relative levels of each protein ultimately determining cell fate (13).

Xenopus is an excellent model to study apoptosis in vertebrate development, as apoptosis is central to metamorphic remodeling (14). Parallel to the essential role of mitochondrial apoptosis in mammalian brain development, some data also point to the mitochondrial route in regulating brain apoptosis during metamorphosis. Such reports include the demonstrations of increases in mRNA encoding XR11, the *Xenopus* homologue to mammalian Bcl-X_L (15), various caspases, including caspase-9 (C9) and caspase-3 (C3) (16, 17), and Apaf1 (D. Du Pasquier, personal communication) in brains of metamorphosing tadpoles. Further, XR11 plays neuron-specific roles in governing neuronal apoptosis, providing one of the few demonstrations of neuron-specific apoptotic programs linked to the mitochondrial death pathway in the metamorphosing nervous system (18).

Given the lack of insight into the mechanisms underlying the action of the mitochondrial pathway in neuronal cell death in amphibia, we examined the role of the *Xenopus* C9 and XR11, two key actors of the mitochondrial pathway, in regulation and maturation of the CNS during *Xenopus laevis* metamorphosis.

By studying phenotypes of single- or double-transgenic tadpoles, we show that C9 and XR11 are implicated not only in regulating apoptosis in the CNS during metamorphosis, but also that they increase numbers of actively proliferating neuroblasts in ventricular brain areas. Moreover, we show that perturbation of the proliferative pool of neuroblasts impacts on brain development, resulting in a modified brain morphology of juvenile *Xenopus*.

Results

Caspase-9 Activation Increases in Tadpole Brain During Metamorphosis. To assess whether C9 is functionally active in metamorphosing *X. laevis* tadpole brains, we used an antibody (17) against active C9 on Western blots of tadpole brains. A 34-kDa band was detected (Fig. 1A), corresponding to conversion of pro-C9 into active C9, as predicted from cleavage sites in the procaspase sequence (17).

The kinetics of C9 activation was monitored on brain extracts at different stages between onset and end of metamorphosis. Fig. 1A shows that active C9 is present before (stage NF55) and during metamorphosis (stages NF57–63). From stages NF57 to NF60, the 34-kDa band intensifies, indicating that active C9 peaks during metamorphosis (stage NF60).

Author contributions: B.A.D. designed research; L.C., K.L.B., and I.R. performed research; L.C., K.L.B., I.R., and B.A.D. analyzed data; and L.C. and B.A.D. wrote the paper.

The authors declare no conflict of interest.

This article is a PNAS Direct Submission.

Abbreviations: RFP, red fluorescent protein; VL, lateral ventricle; 3V, third ventricle; CB, cerebellum; SGT, somatic gene transfer; ISH, *in situ* hybridization.

*To whom correspondence should be addressed. E-mail: demeneix@mnhn.fr.

This article contains supporting information online at www.pnas.org/cgi/content/full/0608877104/DC1.

© 2007 by The National Academy of Sciences of the USA

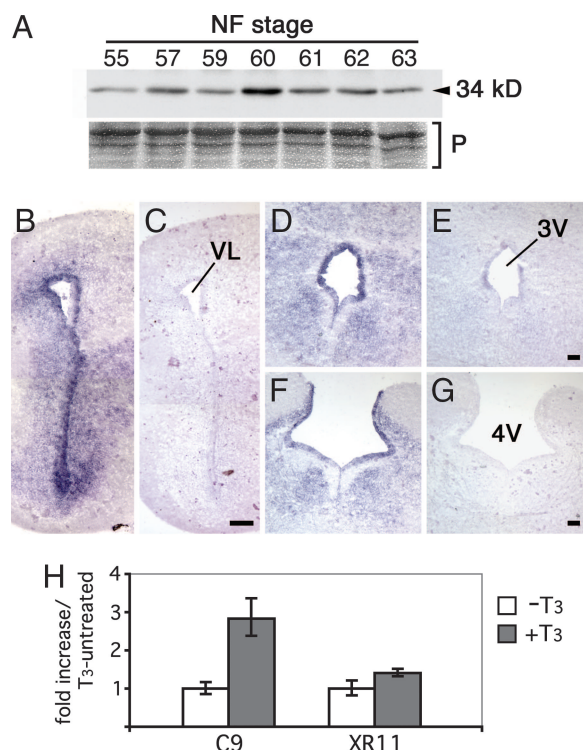


Fig. 1. Caspase-9 mRNA and activated caspase-9 increase in metamorphic tadpole brains. (A) Activation of C9 was monitored by Western blotting on brain extracts of tadpoles at different stages of metamorphosis, by using an active C9 specific antibody. The 34-kDa band, corresponding to conversion of pro-C9 to active C9, as predicted from cleavage sites in the procaspase sequences (17), is seen from stage NF55 (onset of metamorphosis) up to stage NF63 (end of metamorphosis), peaking at stage NF60 (climax of metamorphosis). The immunoblot was repeated by using independent samples. Equal amounts of proteins were loaded per lane and subsequently confirmed by Ponceau-S staining (P). (B–G) Spatial distribution of C9 mRNA in *Xenopus* brains at stage NF63 with ISH, by using an antisense digoxigenin-labeled probe on coronal sections (B, D, and F). Strong localized expression of C9 mRNA is seen in the ventricular zone of the anterior (B), medial (D), and posterior (F) brain. Control adjacent sections were hybridized with a sense probe (C, E, and G), showing no labeling. ISH was done twice on independent groups of tadpoles showing identical results. VL, 3V, and 4V: lateral, third, and fourth ventricles. (Scale bars: B–G, 50 μ m.) (H) Quantitative-PCR analysis of C9 and XR11 expression after T₃-treatment of perchlorated tadpoles. Fold inductions were normalized against untreated tadpoles. Statistical analysis for PCR data were done comparing the means of Δ CT values \pm SD, by using Student's *t* test ($n \geq 3$): Differences were extremely significant for C9 ($P < 0.001$) and significant for XR11 ($P < 0.05$).

Caspase-9 mRNA Is Highly Expressed in the Metamorphosing Tadpole Brain. Next, C9 mRNA distribution was followed during metamorphosis. *In situ* observations show widespread C9 expression in stage NF63 brains [Fig. 1 *B–G*; [supporting information \(SI Fig. 5B\)](#)]. Moreover, C9 expression is marked around the ventricles, zones of active cell proliferation (refs. 19 and 20; see also Fig. 3). Strong expression is found throughout the periventricular areas, from the forebrain [lateral ventricle (VL); Fig. 1*B*] to midbrain (third ventricle; Fig. 1*D*) and hindbrain (fourth ventricle; Fig. 1*F*). Similar distributions, but with weaker signals, were seen at stage NF57 ([SI Fig. 5A](#)). By using quantitative-PCR, C9 and XR11 expression was monitored after T₃ treatment of perchlorated (hypothyroid) tadpoles (Fig. 1*H*). The means of Δ CT quantitative-PCR values were compared by using Student's *t* test. C9 expression increased significantly ($P < 0.001$), as did XR11 expression, but with a lesser fold increase than C9 ($P < 0.05$). Thus, T₃ induces C9 and XR11 expression, confirming the

metamorphic-related increase described previously by Northern blot (15, 16).

C9 distribution in brain was correlated with patterns of apoptosis and proliferation in premetamorphosis (stage NF57; [SI Fig. 5A](#)) and at the end of metamorphosis (stage NF63; [SI Fig. 5B](#)). Generally, TUNEL-positive apoptotic cells map with the C9 expression pattern all over the brain. However, proliferation patterns revealed by using the PH3-mitotic cell marker (21) showed some interesting differences. As expected, mitotic positive cells were largely distributed along ventricle borders, zones of active cell proliferation (19, 20). More interestingly, proliferation was highest at stage NF57, when C9 expression in the periventricular zone was weak ([SI Fig. 5A](#)), whereas, inversely, strongly increased C9 expression in this zone observed at stage NF63 was associated with a major decrease in positive PH3-mitotic cells ([SI Fig. 5B](#)).

Apoptosis Is Reduced in Transgenic Animals Expressing DN9, a Dominant-Negative Form of Caspase-9, and/or XR11, the Bcl-X_L Xenopus Homologue. To gain insight into the role of C9 during *Xenopus* neurogenesis, we used a dominant negative, DN9, fused to red fluorescent protein (RFP) (17). The transgene was expressed from the neuronal-specific promoter N β t, giving N β t-DN9-RFP transgenic animals. In parallel, we investigated the role of another factor linked to the mitochondrial pathway, the antiapoptotic XR11 fused to GFP and N β t-driven (N β t-XR11-GFP), previously analyzed for its role in neuron-specific death in the peripheral nervous system (18).

After crossings, F₁ transgenic tadpoles overexpressing either the dominant negative alone (DN9xDN9), the Bcl-X_L homologue alone (XR11xXR11), or both factors (XR11xDN9) were obtained and their phenotype analyzed.

Apoptosis was examined in WT and transgenic tadpoles by TUNEL labeling on sagittal sections of stage NF61 brains (SI Fig. 6). Widespread distribution of positive apoptotic cells was seen in brains of WT tadpoles. Apoptosis was most marked in the ventral part of the anterior brain, in the subpallium area (SI Fig. 6 *A, B, D, and E*). This ventral distribution in WT anterior brain is also seen on coronal sections at stages NF57 and NF63 (SI Fig. 5 *A and B*). In contrast, apoptosis in XR11xDN9 tadpoles was markedly reduced (SI Fig. 6 *C and F*). Although apoptosis could still be detected throughout the brain, there were fewer TUNEL-positive cells in the subpallium area compared with controls (SI Fig. 6, compare *B'* and *E'* with *C'* and *F'*). A similar decrease in apoptosis was observed in DN9xDN9 and XR11XR11 transgenic animals (data not shown).

Many studies show mutant mice for C3 and C9 share similar brain phenotypes (7, 8). Thus, we examined C3 activity in the same brain region in tadpoles at the end of metamorphosis (stage NF66). Western blots were performed on anterior and posterior brain extracts and C3 activity compared in both extracts for control and transgenic animals by using a specific antibody against active C3 (SI Fig. 7). Variations were seen in active C3 in the anterior and posterior brains of transgenics DN9xDN9 and XR11xDN9 tadpoles, but no anterior/posterior difference was seen in control brains (SI Fig. 7).

Thus, TUNEL labeling and C3 activity were decreased in the anterior brains of transgenic as compared with WT animals, at stages NF61 and NF66, respectively. Taken together, these results show reduced apoptosis, particularly in the forebrain, of transgenic animals overexpressing DN9 and/or XR11.

Mitosis Is Significantly Enhanced in Brains of Transgenic Animals During Metamorphosis. Given the high levels of C9 expression in ventricles during metamorphosis (Fig. 1 and [SI Fig. 5](#)), we investigated the role of DN9 on proliferation in this period. Proliferation was quantified in transgenic lines and compared with controls by using PH3 as a marker of mitosis (Fig. 2).

To better understand the impact of DN9 overexpression by SGT, mitosis was monitored by using PH3 at 3 and 15 days after transfection (Fig. 3). A significant increase in numbers of positive cells for DN9-expressing brains was seen in the VL at 15 days after transfection (Fig. 3 *A–F*). Moreover, the proliferative area was enlarged with higher numbers of PH3 labeled cells lining the ventricle, whereas labeled cells were less frequent in controls (Fig. 3, compare *C* and *F*). Widespread enhancement of PH3 positive cells was also seen throughout the ventricles of DN9 transfected brains, as the SGT technique provides broad transfection of cells lining the brain ventricles (data not shown). Quantifying PH3-positive cells in the VL confirmed the significant enhancement of mitosis in DN9-GFP-transfected brains (Fig. 3*G*). Indeed, cell proliferation increased ≈ 2 -fold after 15 days in tadpoles expressing DN9, an increase correlated with the

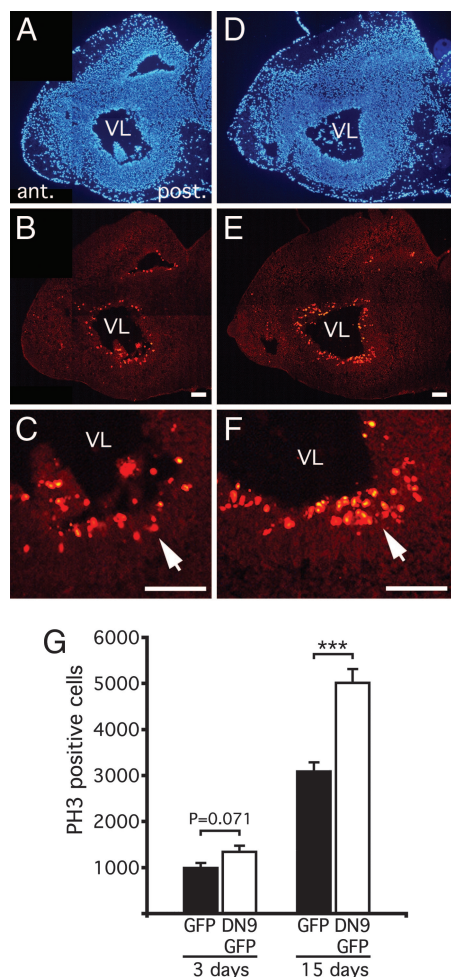


Fig. 3. DN9 expression increases active cell proliferation in the ventricular zone of transfected brain. SGT in brain was carried out at stage NF57 by using CMV-driven DN9-GFP or GFP constructs, and proliferation was compared between DN9 and controls at 3 and 15 days after transfection by using the PH3-antibody. (A–F) Mitotic cells were observed on *para*-sagittal sections at 15 days after transfection for control (B and magnification, C) and compared with DN9 (E and magnification, F), showing more proliferative cells in DN9-transfected brain. DAPI counterstaining shows the same anterior brain region compared with control (A) and DN9 transfections (D). Note at higher magnification the greater concentration of positive cells for DN9 (arrows) lining the ventricle. (G) PH3-positive cells were counted for the VL in the anterior brain, showing a strong increase in mitosis in brains transfected with DN9 vs. controls. Each experiment was repeated twice, giving similar results. Means \pm SEM are given; $n > 6$ in each group; ***, $P < 0.001$. (Scale bars: A–F, 100 μ m.)

high luciferase ratio (value = 8.5) seen at this time (compare Fig. 3G and SI Fig. 8E).

Brain Morphology of Metamorphosed Transgenic Animals Is Modified by DN9 and/or XR11 Expression. At stage NF66, after metamorphosis, overall brain morphologies of each transgenic line were compared with WT (Fig. 4). Although the length and maximum width of the whole brain did not change in transgenics, the relative brain proportions were markedly modified (see Fig. 4*I* for a schema of the anterior brains of controls and the transgenic lines). In transgenics, the forebrain was more compact, particularly for the double-transgenic XR11xDN9 (Fig. 4*J*). Other morphological differences included more pronounced commissures in WT at the forebrain/midbrain and forebrain/olfactory bulb junctions and more prominent CB in transgenics (Fig. 4*A–H*).

Discussion

Apoptosis is crucial to normal CNS development. Perturbation of regulation or execution of apoptosis dramatically affects brain development in mammals (for reviews, see refs. 4 and 23). We used *Xenopus* tadpoles to investigate the mechanisms maintaining the balance between cell death and proliferation during metamorphosis, a period comparable to the mammalian perinatal phase (24, 25).

We show that C9 mRNA is highly expressed in the neurogenic ventricular region during metamorphosis, and that neuronal-specific expression of DN9, a dominant negative against C9, reduces brain apoptosis. DN9 markedly modifies the equilibrium of proliferation and death, specifically in the neurogenic ventricular region, stimulating strong activation of mitosis throughout metamorphosis. Further, modulation of other actors in the mitochondrial apoptotic pathway, namely, *Xenopus* XR11 (the homologue of mammalian Bcl-X_L) produces a similar phenotype, that of increased numbers of actively proliferating cells and changes in overall brain morphology.

These findings confirm a central role for the mitochondrial route during morphogenesis of the developing amphibian brain. In particular, morphological remodeling is most evident in the anterior brain of DN9 and XR11 transgenics (Fig. 4I). Interestingly, it is also the forebrain that shows the most dramatic defects in C9 mutant mice, as well as for C3 and Apafl mutant mice (26–28). Despite these marked changes in the CNS, no changes have been noted in the peripheral nervous system for these mice. Similarly, there was no modification of motoneuron death in the lateral motor column of XR11xDN9 *Xenopus* (data not shown), as seen for Nβt-XR11 animals (18), corroborating data in mice showing that C9 or C3 deletion does not modify elimination of spinal cord motoneurons (27, 29, 30).

The pattern of *Xenopus* C3 expression suggests that it, too, contributes to the regulation of neuronal death, as for C3-null mutant mice. The fact that active C3 was decreased in anterior brain for DN9 and XR11 transgenic animals suggests strongly that C3 is implicated in the transmission of death signals initiated by mitochondria in brain. The preponderant role of this caspase in apoptosis in mouse brain has been described in previous studies, demonstrating that this enzyme is a key actor in the regulatory proteolytic cascade in the CNS (26, 31). Moreover, the role of C3 seems to be more pronounced in the anterior tadpole brain, as this area is most affected when DN9 and XR11 are overexpressed. This observation could explain why morphological alterations are found mainly in the forebrain of post-metamorphic transgenic tadpoles.

C9 mRNA expression shows strong labeling in ventricular cells and the active form of C9 increased transiently during metamorphosis, with a peak at metamorphic climax (Fig. 1 and SI Fig. 9). Remarkably, increased C9 activity is correlated with decreased cell proliferation. Moreover, when DN9 (and/or XR11) are overexpressed, the most marked effect on proliferation is seen at climax, when active C9 is normally maximum (SI Fig. 9). Thus, expression of DN9 (and/or XR11) maintains proliferation, whereas the normal levels of C9 dampen proliferative levels. This suggests an important and specific role for C9 (and also XR11) controlling neuronal cell proliferation during the critical period of metamorphosis. The SGT experiments confirm that C9 can be a major player in maintaining the balance between cell death and proliferation. Indeed, when DN9 expression is limited by SGT to the neurogenic zone, where C9 is normally expressed, it results in increased mitosis. We infer that this effect results from inactivation of C9-dependent pathway, suggesting a direct effect of DN9 on this neurogenic population.

Finally, DN9 and XR11 overexpression does not simply abrogate apoptosis but also maintains the neurogenic pool in a proliferative state as we observed an increased rate of mitosis in

the neuroblast population. Indeed, cell number is controlled by an intricate balance of cell death and cell proliferation. Deregulation of the apoptotic/proliferative balance leads to impaired development and many diseases including neurodegenerative disorders, viral infections, and tumors. It is clear that links between apoptosis and cell cycle control mechanisms exist and close interactions between factors implicated in cell cycle progression and pro- or anti-apoptotic factors implicated in death pathways have been reported (32–35). Recently, it was shown that transgenic ES cell lines expressing Bcl-2 in presence of Leukemia Inhibitory Factor were sufficient to allow expansion of these mouse pluripotent stem cells *in vitro*, even in the absence of bone morphogenic proteins, underlying the close link existing between the maintenance of a proliferative state and the Bcl-2 factors implicated in the regulation of apoptotic processes (36).

Here we show that C9 and XR11 contribute to regulate both apoptosis and cell proliferation in the ventricular zone and perturbation of their expression leads to the modification of regulation of cell cycle of neuroblasts, with distinct consequences on final brain morphology.

Elucidating the mechanisms that link cell cycle control with apoptosis, and their regulation, will be important in understanding development of the nervous system and how neuronal cells do or do not evade these constraints, and thereby prevent uncontrolled proliferation. *Xenopus* could represent a useful model for analyzing these intricate mechanisms, particularly during metamorphosis, which is simultaneously associated with apoptosis, proliferation and differentiation. Future work could be directed toward identifying more precisely in the neurogenic zone, and using specific cell markers, which cell type(s) are directly affected by DN9 and XR11 overexpression.

In summary, our data provide *in vivo* evidence for a direct implication of C9 and XR11, two key regulators of the mitochondrial death pathway, in regulating the balance between neuronal apoptosis and proliferation in metamorphosing brain. To our knowledge, this report provides a previously undescribed role of specific apoptotic actors in modifying the outcome of metamorphic neurogenesis and brain remodeling.

Materials and Methods

Animals. *X. laevis* tadpoles were raised as described (17) and staged according to Nieuwkoop and Faber (37). Animals were killed by decapitation after anesthesia. All animal studies were conducted according to the principles and procedures described in Guidelines for Care and Use of Experimental Animals.

C9 and DN9 Constructs. Cloning of *Xenopus tropicalis* C9, mutation to DN9, and fusion to RFP (DN9-RFP) have been described (17). The RFP marker in CMV-DN9-RFP was replaced with GFP, giving the CMV-DN9-GFP construct. The pEGFP-C3 (as CMV-GFP) and pDsRed2-N1 (as CMV-RFP) vectors (Clontech, Ozyme, St. Quentin en Yveline, France) were used in control experiments. For transgenesis, the CMV promoter in CMV-RFP and CMV-DN9-RFP constructs was replaced by the Nβt promoter (18), giving the Nβt-RFP and the Nβt-DN9-RFP constructs.

SGT in Brain. SGT in brain used a PEI-based method (22). For each injection (1 μl), 0.1 μg of pcDNA3-Luc (LUC plasmid) was coinjected with 0.4 μg of CMV-GFP or CMV-DN9-GFP constructs. *In toto* GFP labeling was observed on brains before luciferase activity was monitored on brain extracts by using a Luciferase Kit (Promega, Charbonnières, France).

Germinal Transgenesis. Transgenesis was carried out according to the modified Kroll and Amaya protocol (18). For each transgenesis, 200 ng of ApaLI-linearized constructs was used. Transgenic animals were obtained for Nβt-RFP and Nβt-DN9-RFP

